

# MONTE CARLO SIMULATIONS OF X-RAY GENERATION AND DETECTION

Maurício Moralles<sup>1</sup>, Carla da Costa Guimarães<sup>2</sup> e Emico Okuno<sup>2</sup>

1-Instituto de Pesquisas Energéticas e Nucleares - IPEN-CNEN/SP  
Caixa Postal 11049, CEP 05422-970, São Paulo, SP, Brasil

2-Instituto de Física da Universidade de São Paulo  
Caixa Postal 66318, CEP 05315-970, São Paulo, SP, Brasil

## ABSTRACT

The employment of Monte Carlo simulations in the applied nuclear physics techniques has increased with the data processing capabilities of the commercial personal computers. Since the inclusion of the low-energy electromagnetic interactions in GEANT4, this Monte Carlo simulation toolkit has produced results which reveal its promising utilization in radiation dosimetry, radiation protection and medical applications. With the GEANT4 toolkit, interactions of electrons and photons with matter can be simulated down to energies as low as 250 eV. The present work shows simulation results of X-ray generation from a typical X-ray tube by impinging electrons on a tungsten target, and filtering the produced photon beam with a beryllium window. In this process, characteristic and bremsstrahlung radiation are produced. Rayleigh, Compton, photoelectric and pair production interactions can be included in the transport of photons through the environment. The spectral analysis of the photon beam is performed by simulating a cadmium zinc telluride detector positioned in the radiation field. Different filters can also be placed in the radiation field to produce the desired attenuation. Comparisons with experimental data show that the simulated spectra reproduce very well the reality, indicating that the GEANT4 toolkit can be a good choice for future simulations of experimental conditions for dosimetric purposes, such as dosimeter responses and dose estimations

Keywords: X-ray, monte carlo, GEANT 4.

## I. INTRODUCTION

The use of ionizing radiation is presently very common in several areas, being the most important in medical procedures. Applications of radiation demand precise knowledge of both, the radiation characteristics and the amount of energy deposited in the environment. Precise calculations of production and transport of radiation in any material is feasible, in principle, since the interactions of radiation with matter are well understood and there is enough data of cross-section for these interactions. However, most of the physical systems which are subject to radiation have inherent difficulties to be simulated, due to geometrical complexity and the presence of different materials, like the problems treated in radiation dosimetry, radiation protection and medical physics. For such calculations, the Monte Carlo method is recommended and the precision obtained in the simulations depends much on the computation time. Nowadays, detailed Monte Carlo simulations are possible with the new generation of personal computers, which have high data processing capabilities.

Several Monte Carlo codes have been developed to perform calculations of interactions of radiation with matter

and one of them is GEANT4, which is a product of a world-wide collaboration initiated in the European Organization for Nuclear Research (CERN). GEANT4 is a freely distributed package, written in C++ language, which provides a set of tools for Monte Carlo simulations of nuclear and high energy physics experiments[1]. It contains the basis for virtual building of physical systems with several geometric forms and permits the inclusion of practically all materials. GEANT4 provides the necessary interactions of particles with matter in a wide energy range. The interest in simulations involving low-energetic electrons and photons led the GEANT4 developers to include a low-energy extension of electromagnetic interactions[2]. The cross-sections data used by GEANT4 allow precise calculation of interactions of particles with energies as low as 250 eV.

In the particular case of X-ray dosimetry, simulations connected to the response of dosimeters demand the best possible description of the radiation field in the energy range of hundreds of eV up to several MeV. The employment of a new simulation code must be tested by comparisons with results of experiments.

The present work describes studies of generation, filtering and detection of X-rays by using the GEANT4 toolkit. Two C++ applications were written: the first one simulates the X-ray beam produced by a typical tube, and the second one, the measured X-ray spectra by a cadmium zinc telluride detector placed in the radiation field. The simulation results are compared with experimental data obtained in the similar conditions.

## II. THE EXPERIMENTAL SETUP

The X-ray beams were produced by a Philips tube (type MG 450) with a tungsten rotating anode. The electrons hit the anode at an angle of  $22^\circ$  and a fraction of produced photons cross a 2.2 mm beryllium window before leaving the tube. The photon beam has a divergence angle of  $30^\circ$ . Different filters can be employed to attenuate the photon beam to obtain the radiation with desired quality.

A cadmium zinc telluride (CZT) detector was used to measure the X-ray spectra for different combinations of electron accelerating potential (kVp) and filters. The CZT detector (type AMPTEK XR-100T-CZT) has a beryllium window with 250  $\mu\text{m}$  thickness and a  $\text{Cd}_{0.9}\text{Zn}_{0.1}\text{Te}$  crystal with a volume of  $3 \times 3 \times 2 \text{ mm}^3$ . The detector was positioned at the distance of 6 meters from the X-ray tube. A tungsten collimator, with an aperture of 400  $\mu\text{m}$  and thickness of 2.0 mm, was placed in front of the detector window to maintain the counting rate at convenient levels. Too high counting rates can produce undesirable effects, like the pile up of pulses, which deteriorate the quality of the measured spectrum. Fig. 1 shows the experimental setup. The energy response of the CZT detector was calibrated with a standard  $^{133}\text{Ba}$  source.

## III. THE MONTE CARLO SIMULATION

The experimental arrangement has large dimensions in comparison with the points where the X-ray production and detection occur. Photons are produced in a small spot on the tungsten target and are detected by a  $9 \text{ mm}^2$  surface. The solid angle of the detector is very small and the simulation of the performed measurements must be carried out in two steps. In the first step, the production of X-ray by the tube is simulated and the photon spectrum is recorded for each kVp value. In the second step, the emission and filtering of a X-ray beam is simulated. The photon spectrum obtained in the first step is the input for the calculations of the energy distribution of the photons emitted by a source in the second step, and the detector is placed inside a small solid angle.

The simulations in both steps employ the low-energy electromagnetic interactions provided by the GEANT4 toolkit. Electrons interact with matter via bremsstrahlung and ionization, while photons, via Rayleigh effect, Compton scattering and photoelectric effect. The decay of ionized atoms takes into account fluorescence as the relaxation process of excited atoms. According to the GEANT4 developers, the low-energy extension of the electromagnetic processes is precise for energies down to

250 eV and covers elements with atomic numbers from 1 to 99. The employed cross sections, stopping powers and atomic data have been taken from publicly distributed data libraries[3-6].

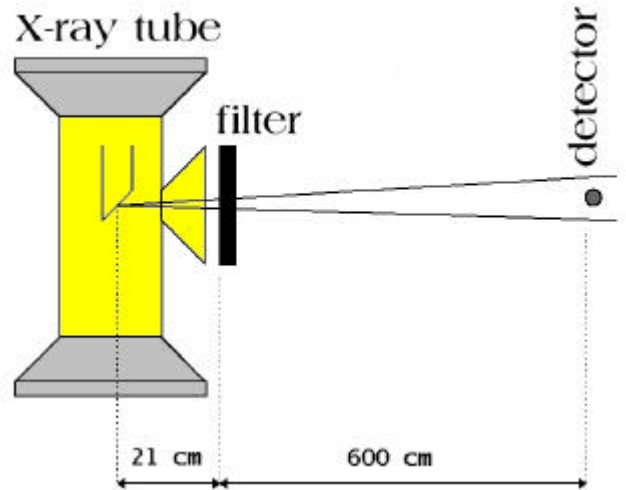


Figure 1. Scheme of the experimental setup used in the measurements of spectra produced by the X-ray tube.

**Simulation of X-ray generation.** The simulation of the X-ray generation comprises an electron gun, a target and a filter placed in a vacuum chamber. In the simulation, these parts are small in comparison to the real ones for reasons of computation time. The miniaturization of the tube should not affect the final spectrum of the generated photons, considering that the dimensions of the target are enough to stop all electrons. A scheme of the arrangement used to simulate the generation of X-rays is shown in Fig. 2.

The electron gun is dimensionless. It consists of a point in space from where electrons are emitted with energy of fixed value, corresponding to the simulated kVp. Electrons are emitted in a straight line, directed to the target surface.

The target is a cylinder made of tungsten with thickness of 5.0 mm and radius of 2.0 mm. Its surface makes an angle of  $22^\circ$  with the beam line of the electron gun.

The filter is made of a beryllium disk with thickness of 2.2 mm and radius of 1.1 cm, placed at 1.0 cm from the point where the electrons hit the target. This piece should simulate the beryllium window of the tube.

The energy of photons are recorded when they cross a surface placed at 1.5 cm from the target, indicated by "photon analyzer" in Fig. 2. Figure 3 shows a simulated spectrum (number of photons/electrons) for electrons with energies of 180 keV. In the inset, one can see the characteristic X-ray lines of tungsten with more details. Figure 4 shows spectra produced by 100, 80, 40 and 25 keV electrons.

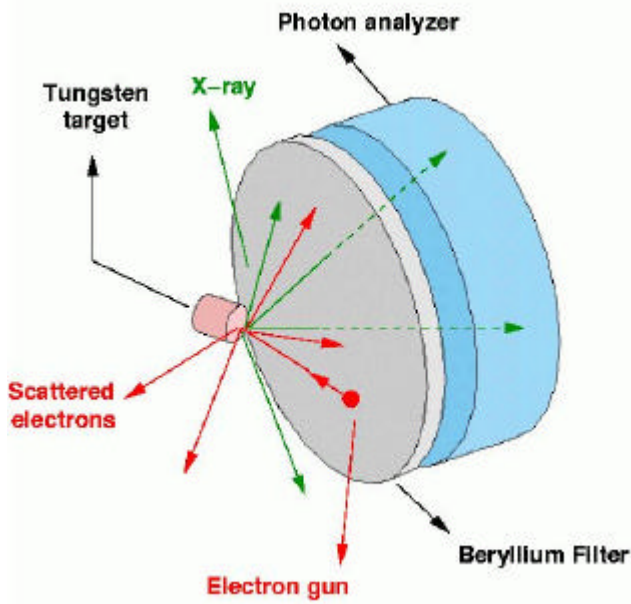


Figure 2. Scheme of the configuration used in the simulation of X-ray generation. Electron and X-ray tracks are represented in red and green, respectively.

**Simulation of X-ray detection.** The elements included in the simulation of the X-ray detection were a photon source, filters, a collimator and a CZT crystal. All pieces are placed inside a cylindrical chamber filled with air.

Photons are emitted with energy distributions given by the spectra produced in the simulation of X-ray generation. Their directions are randomly distributed inside a fixed solid angle. Filters are disks placed at 21 cm from the source. The detector is placed inside the solid angle of the beam, 6 m from the source, and has a tungsten collimator in front of its beryllium window. A cylindrical piece of aluminium, 1.5 cm thick, is placed behind the CZT crystal to simulate the crystal support.

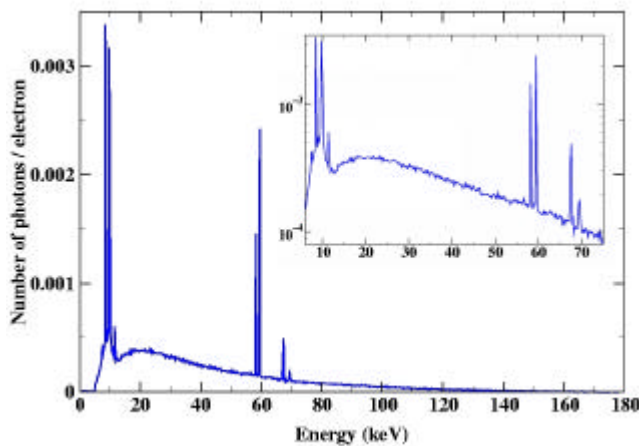


Figure 3. X-ray spectrum obtained by simulation with 180 keV electrons impinging on a tungsten target. The inset shows an enlargement of the 10 keV - 70 keV region.

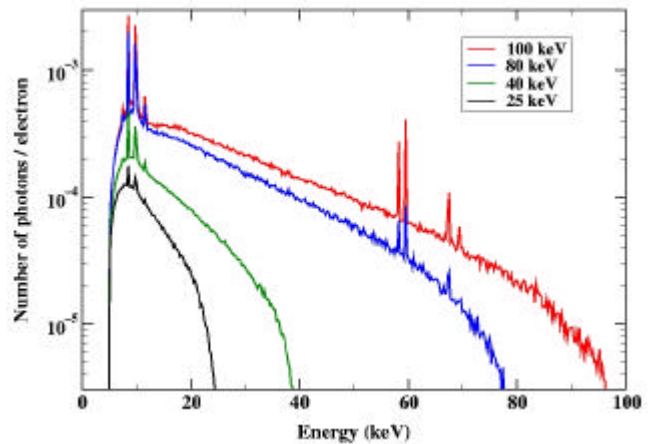


Figure 4. X-ray spectra obtained by simulation with electrons impinging on a tungsten target. Electron energies: 100 keV (red), 80 keV (blue), 40 keV (green) and 25 keV (black).

The calibration spectrum obtained with the  $^{133}\text{Ba}$  source was also simulated. In this case, the energy distribution of photons was taken from the experimental probabilities of X-ray and gamma radiation following the decay of  $^{133}\text{Ba}$  [7]. The dependence of the energy resolution of the detector with the photon energy was calibrated using a linear function. This calibration was used to include a Gaussian dispersion in the simulated data. The scheme of the arrangement used in the simulation of the photon detection is presented in Fig. 5.

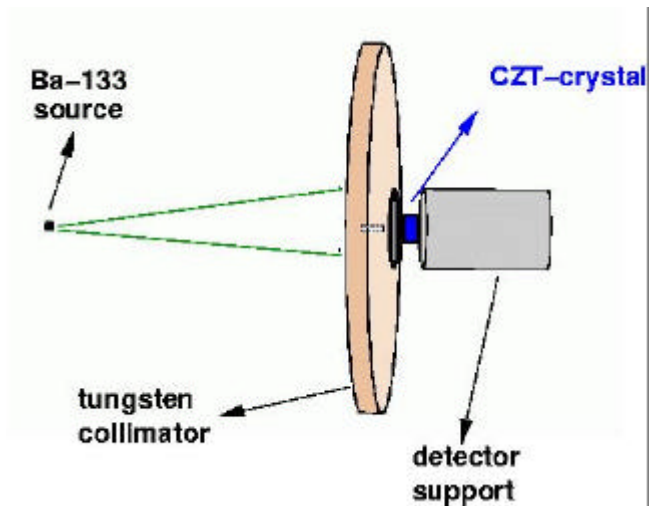


Figure 5. Scheme of the parts used in the simulation of the photon detection.

#### IV. COMPARISON WITH EXPERIMENTAL RESULTS

Before analysing the simulated and experimental results, some particular aspects concerning the CZT detector must be considered.

Due to the trapping of charge carriers inside the CZT crystal, the charge collection is less efficient when the electron-hole pairs are created near the cathode. This effect makes the response of the detector dependent on the position where the radiation loses its energy. Most of the events with incomplete charge collection are rejected during the electronic analysis of the amplified pulses. The net effect of this rejection is that the active volume of the crystal depends on the radiation energy[8]. Since this dependence was not taken into account in the simulations, great differences between experiment and simulation are expected for spectra with wide energy range. The inclusion of a model which takes into account the charge collection have been reported in the literature[9] and can be implemented in our simulation code in the future.

**Calibration source.** Experimental and simulated spectra of the calibration source are presented in Figs. 6a and 6b, with the discrete emissions of  $^{133}\text{Ba}$  in the 30 keV - 380 keV range. The general agreement between simulated and measured spectra is reasonable, but some differences due to effects of incomplete charge collection are observable by comparing the relative intensities of photopeaks. The correspondence of relative intensities in the high energy region (Fig. 6b) is very good. The active volume of the detector for these photopeaks in the range of 276 keV to 384 keV is practically the same, i.e. the rise-time rejection have similar effects in this energy region. The low-energy region (Fig. 6a) presents the charge collection problem, as can be observed by comparing the 81 keV photopeak intensities. The region from 10 keV to 100 keV, in particular, is more sensitive to this effect because the absorption of photons by the CZT detectors in this energy range is close to 100% [8].

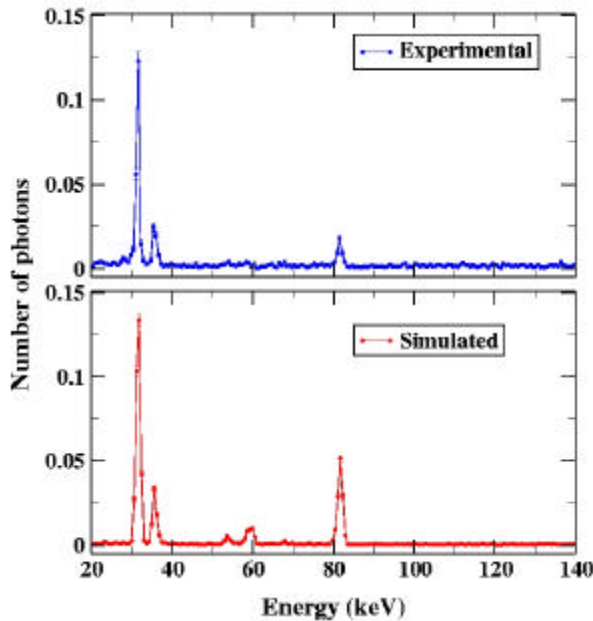


Figure 6a. Normalized experimental and simulated spectra obtained with a  $^{133}\text{Ba}$  source. Energy range: 20 keV to 140 keV.

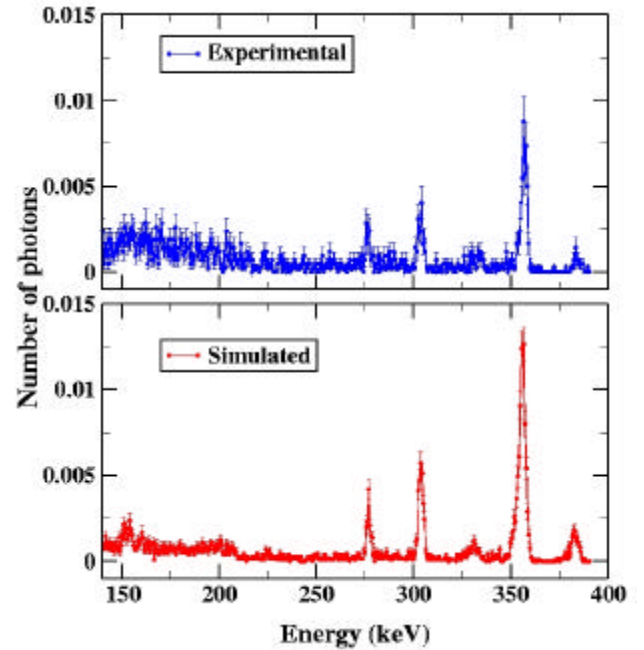


Figure 6b. Normalized experimental and simulated spectra obtained with a  $^{133}\text{Ba}$  source. Energy range: 140 keV to 400 keV.

**Filtered X-ray source.** Normalized spectra for three combinations of kVp and filters are shown in Figs. 7, 8 and 9. One should notice that the density of plotted points are 1.6 and 4.0 points/keV in the experimental and simulated spectra, respectively. The small peaks at the left side of the experimental spectra are originated by electronic noise.

The energy ranges in the simulations with the X-ray tube are narrower than in the  $^{133}\text{Ba}$  source. The simulated and experimental spectra have similar shapes, but some differences are observed when the mean-energy values are compared. Table 1 presents the mean-energy values of the simulated and experimental spectra. The noise region was excluded in the mean-values calculations. The simulated spectra for kVp = 80 kV (Fig. 7) and 100 kV (Fig. 8) agree very well with the experimental one, showing small difference of intensity in the 20 keV - 35 keV energy range in the latter. The differences in the low-energy region of the spectrum obtained with kVp = 180 kV are more pronounced. The mean-energy value differ in almost 8 keV for this wide energy range spectrum, as a consequence of the greater number of events in the region between 15 keV and 45 keV in the experimental spectrum.

## V. CONCLUSIONS

Generation, filtering and detection of X-rays were simulated using the GEANT4 Monte Carlo toolkit. Models for typical X-ray tube and solid-state detector were employed. Good agreement between simulated and experimental results was obtained, using a very simple model to describe a CZT detector. These results show that GEANT4 is adequate for simulations with low-energy electromagnetic interactions.

Major differences between experimental and simulated results were observed for wide energy range, which can be attributed to events subject to imperfect charge collection in the detector. More realistic simulations must use a model that includes the rejection of interactions near the cathode, in order to describe the rise-time rejections of the CZT detector.

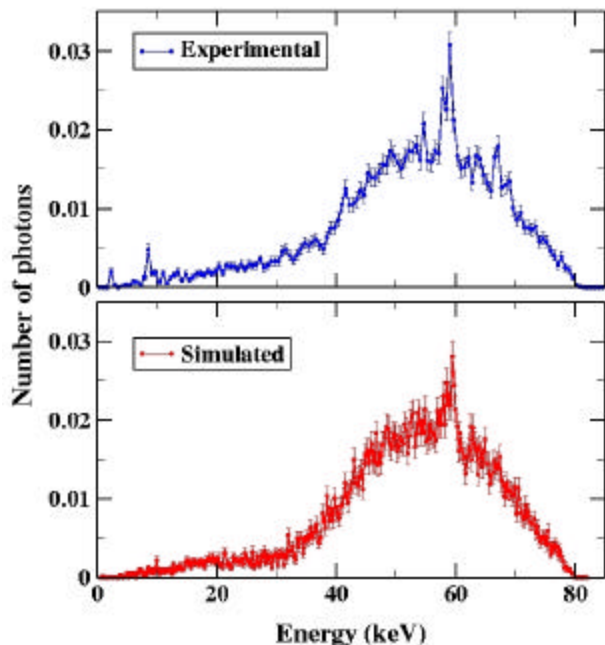


Figure 7. Normalized experimental and simulated spectra obtained with kVp = 80 kV and filtering with 0.5 mm of copper + 4.0 mm of aluminium.

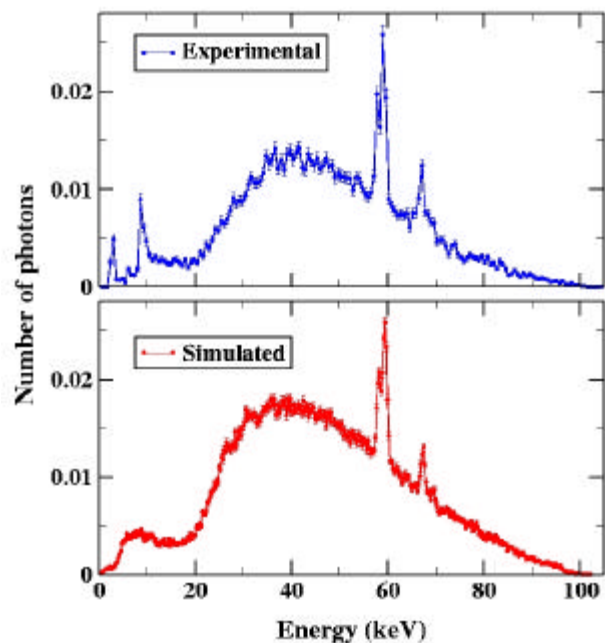


Figure 8. Normalized experimental and simulated spectra obtained with kVp = 100 kV and filtering with 4.0 mm of aluminium.

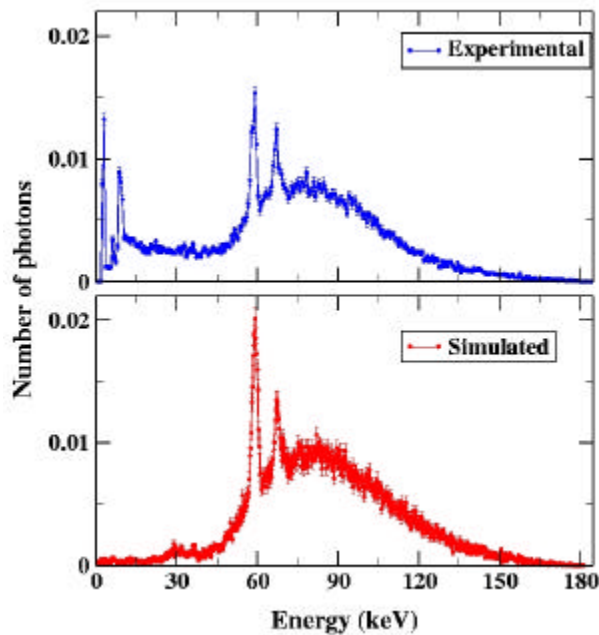


Figure 9. Normalized experimental and simulated spectra obtained with kVp = 180 kV and filtering with 0.4 mm of tin + 0.25 mm of copper + 1.0 mm of aluminium.

TABLE 1. Mean energies of the spectra presented in Figs. 7, 8 and 9, with kVp-values of 80, 100 and 180 kV, respectively .

kVp [kV]	mean energy (experimental) [keV]	mean energy (Monte Carlo) [keV]
80	53.5	53.0
100	48.7	47.8
180	76.4	84.1

## REFERENCES

- [1] Amako, Katsuya, **Present Status of GEANT4**, Nuclear Instruments and Methods in Physics Research, A 453, p 455-460, 2000.
- [2] Agostinelli, S. et al., **Medical applications of the GEANT4 toolkit**, INFN/AE-00/08, SIS-Pubblicazione, Laboratori Nazionale di Frascati, Italy, 2000.
- [3] Cullen, D., Hubbell, J.H. and Kissel, L., **EPDL97: the evaluated photon data library, '97 version**, UCRL-50400, vol. 6, rev. 5, Lawrence Livermore National Laboratory, USA, 1997.
- [4] Perkins, S.T., Cullen, D. and Seltzer S.M., **Tables and graphs of electron -interaction cross sections from 10 eV to 100 GeV derived from the LLNL evaluated electron data library (EEDL), Z=1-100**, UCRL-50400, vol. 3, Lawrence Livermore National Laboratory, USA, 1991.

[5] Perkins, S.T. et al., **Tables and graphs of atomic subshell and relaxation data derived from the LLNL evaluated atomic data library (EADL), Z=1-100**, UCRL-50400, vol. 30, Lawrence Livermore National Laboratory, USA, 1991.

[6] Scofield, J.H., **Radiative Transitions**, Atomic inner-shell process, p 265-292, edited by B. Crasemann, Academic Press, New York, 1975.

[7] Rab, Shaheen, **Nuclear Data Sheets Update for A = 133**, Nuclear Data Sheets, vol. 75, p 491-665, 1995.

[8] Redus, B., **Efficiency of XR-100T-CZT detectors**, AMPTEK Applications Note, ANCZT-1 rev. 1, AMPTEK inc., Bedford, USA, 2000.

[9] Matsumoto, M. et al., **Direct measurement of mamographic x-ray spectra using a CdZnTe detector**, Medical Physics 27, p 1490-1502, 2000.